

■ **CARTILAGE**

# A mutation in *SLC20A2* (c.C1849T) promotes proliferation while inhibiting hypertrophic differentiation in ATDC5 chondrocytes

Y. Li,  
X. Lin,  
M. Zhu,  
F. Xun,  
J. Li,  
Z. Yuan,  
Y. Liu,  
H. Xu

From Guangzhou  
Women and Children's  
Medical Center,  
Guangzhou, China

**Aims**

This study aimed to investigate the effect of *solute carrier family 20 member 2* (*SLC20A2*) gene mutation (identified from a hereditary multiple exostoses family) on chondrocyte proliferation and differentiation.

**Methods**

ATDC5 chondrocytes were cultured in insulin-transferrin-selenium medium to induce differentiation. Cells were transfected with pcDNA3.0 plasmids with either a wild-type (WT) or mutated (MUT) *SLC20A2* gene. The inorganic phosphate (Pi) concentration in the medium of cells was determined. The expression of markers of chondrocyte proliferation and differentiation, the Indian hedgehog (Ihh), and parathyroid hormone-related protein (PTHrP) pathway were evaluated by quantitative real-time polymerase chain reaction (qRT-PCR) and western blotting.

**Results**

The expression of *SLC20A2* in MUT group was similar to WT group. The Pi concentration in the medium of cells in MUT group was significantly higher than WT group, which meant the *SLC20A2* mutation inhibited Pi uptake in ATDC5 chondrocytes. The proliferation rate of ATDC5 chondrocytes in MUT group was greater than WT group. The expression of aggrecan (Acan),  $\alpha$ -1 chain of type II collagen (COL2A1), and SRY-box transcription factor 9 (SOX9) were higher in MUT group than WT group. However, the expression of Runt-related transcription factor 2 (Runx2),  $\alpha$ -1 chain of type X collagen (COL10A1), and matrix metalloproteinase 13 (MMP13) was significantly decreased in the MUT group. Similar results were obtained by Alcian blue and Alizarin red staining. The expression of Ihh and PTHrP in MUT group was higher than WT group. An inhibitor (cyclopamine) of Ihh/PTHrP signalling pathway inhibited the proliferation and restored the differentiation of chondrocytes in MUT group.

**Conclusion**

A mutation in *SLC20A2* (c.C1948T) decreases Pi uptake in ATDC5 chondrocytes. *SLC20A2* mutation promotes chondrocyte proliferation while inhibiting chondrocyte differentiation. The Ihh/PTHrP signalling pathway may play an important role in this process.

**Cite this article:** *Bone Joint Res* 2020;9(11):751–760.

**Keywords:** *SLC20A2*, Phosphate, Chondrocyte, Proliferation, Differentiation

Correspondence should be sent to  
YiQiang Li; email:  
liyiq@gwcmc.org

doi: 10.1302/2046-3758.911.BJR-  
2020-0112.R1

*Bone Joint Res* 2020;9(11):751–  
760.

**Article focus**

- The effect of mutation in *solute carrier family 20 member 2* (*SLC20A2*) (c.C1948T) on inorganic phosphate (Pi) uptake of the ATDC5 cells.
- The effect of mutation in *SLC20A2* (c.C1948T) on chondrocyte proliferation and differentiation.
- The effect of mutation in *SLC20A2* (c.C1948T) on the Indian hedgehog (Ihh)/parathyroid hormone-related protein (PTHrP) signalling pathway.

### Key messages

- A mutation in *SLC20A2* (c.C1948T) decreases Pi uptake of the ATDC5 cells.
- A mutation in *SLC20A2* (c.C1948T) promotes chondrocyte proliferation while inhibiting chondrocyte differentiation.
- *Ihh*/PTHrP signalling pathway may play an important role in the *SLC20A2* mutation-induced disturbance of chondrocyte proliferation and differentiation.

### Strengths and limitations

- We identified a novel mutation in *SLC20A2* gene and found that this mutation promotes chondrocyte proliferation while inhibiting chondrocyte differentiation by decreasing Pi uptake.
- The present study is a cellular experiment, thus animal models with *SLC20A2* mutation (c.C1948T) are needed to further investigate the effect of *SLC20A2* on chondrocyte proliferation and differentiation in vivo.

### Introduction

Hereditary multiple exostoses (HME) is a dominantly inherited childhood disease with an incidence of 1/50,000.<sup>1,2</sup> The clinical manifestations of HME are exostoses on the metaphysis of bones, including the distal femur, proximal tibia, fibula, and humerus, which could lead to local deformity or pathological fractures.<sup>2,4</sup> Although 70% to 95% of cases of HME are associated with mutations in the *exostosin-1* (*EXT-1*) and *exostosin-2* (*EXT-2*) genes,<sup>5,7</sup> there are many patients with HME without *EXT-1* and *EXT-2* gene mutations.<sup>8,9</sup>

In our recent study, we performed whole-exome sequencing in a typical Chinese HME family without *EXT-1* and *EXT-2* mutations and identified a novel mutation of the *solute carrier family 20 member 2* (*SLC20A2*) gene (c.C1849T).<sup>10</sup> As a member of the *SLC20* family of solute carriers, the *SLC20A2* protein (PiT-2) comprises 652 amino acids, and its molecular mass is 70,392 Da.<sup>11</sup> PiT-2 is expressed ubiquitously in all tissues and is considered as a 'housekeeping' transport protein.<sup>11</sup> It is a type III sodium-phosphate (NaPi-III) cotransporter that mediates the transmembrane movement of sodium and inorganic phosphate (Pi).<sup>11-13</sup>

It is well known that Pi is an essential component of all living organisms and must be actively transported into cells across the cell membranes. Cells get Pi in the form of negatively charged Pi from the extracellular environment by secondary active transport.<sup>13</sup> Pi transporters (such as PiT-2) use the inwardly directed electrochemical gradient of Na<sup>+</sup> ions which is established by the Na<sup>+</sup>-K<sup>+</sup>-ATPase, to drive Pi influx into the cells.<sup>13,14</sup> It has been reported that *SLC20A2* variants cause dysfunctional Pi transport activity in endothelial cells,<sup>15</sup> leading to primary familial brain calcification.<sup>15,16</sup>

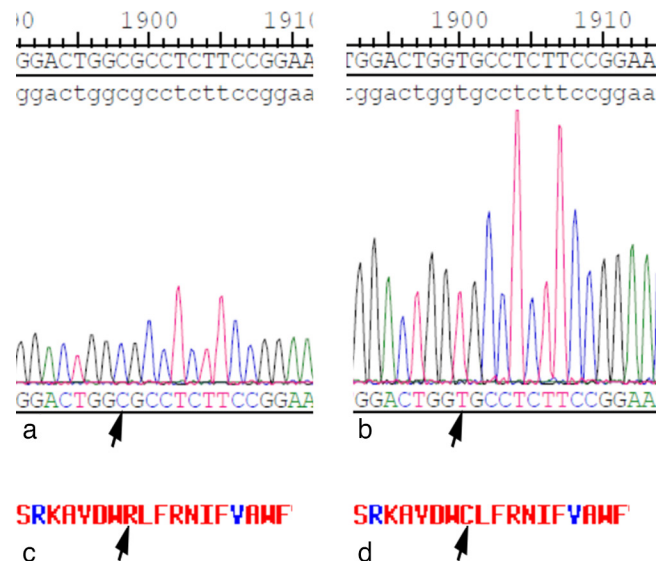


Fig. 1

Sanger sequencing confirmed the a) cloned wild-type and b) mutant mouse *solute carrier family 20 member 2* (*SLC20A2*) complementary DNA (cDNA) (NM\_011394). c) and d) This mutation causes a change of an amino acid in *SLC20A2* protein (R > C). The arrows indicate the site of variance.

In theory, mutation in *SLC20A2* (c.C1849T) may lead to a change in the amino acid sequence (p.R617C) (Figures 1c and 1d),<sup>10</sup> which might induce structural changes and dysfunction of PiT-2, subsequently leading to a disturbance of Pi homeostasis in cells.

Studies have found that HME is characterized by inappropriate chondrocyte proliferation and bone growth arising at the juxtaepiphyseal region of long bones.<sup>17,18</sup> It is well known that Pi plays an important role in the regulation of chondrocyte proliferation and differentiation.<sup>19,20</sup> As *SLC20A2* variants may cause dysfunctional Pi transport activity, we speculated that mutation of the *SLC20A2* gene might induce metabolic disturbance of Pi and inappropriate proliferation and differentiation of chondrocytes, and subsequently lead to development of HME. Additionally, the Indian hedgehog (*Ihh*)/parathyroid hormone-related protein (PTHrP) signalling pathway has been demonstrated to play notable roles in regulating the proliferation and differentiation of chondrocytes.<sup>21-24</sup> Thus, we wanted to verify the effect of the *Ihh*/PTHrP signalling pathway in *SLC20A2* mutation-induced abnormal proliferation and differentiation of chondrocytes.

The ATDC5 cell line, which is derived from mouse teratocarcinoma cells and characterized as a chondrogenic cell line and undergoes a sequential process analogous to chondrocyte differentiation, has been reported to be an excellent in vitro model cell line for skeletal development.<sup>25,26</sup> In this study, we established an ATDC5 cell model with a mutation of *SLC20A2*, aiming to investigate the effect of *SLC20A2* mutation on

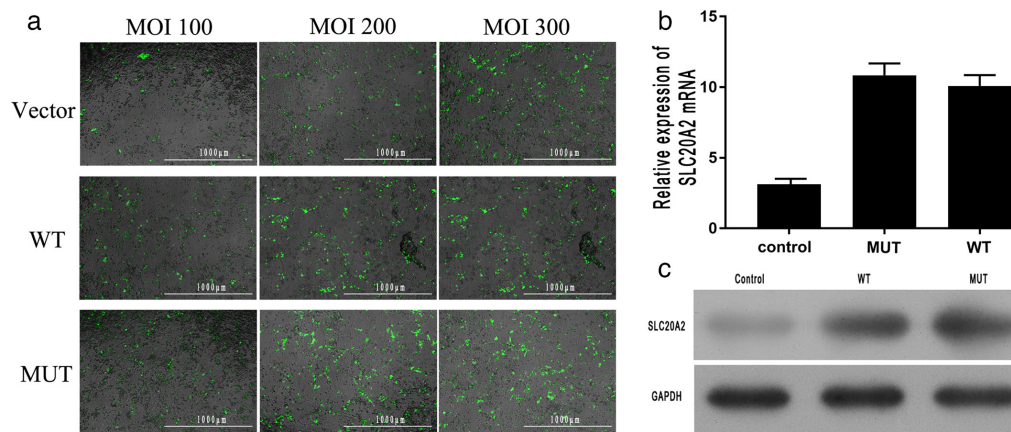


**Fig. 2**

a) An immunofluorescence examination (magnification: 40 $\times$ ) was performed to determine the transfection efficiency of the cell lines. Three different quantities of pcDNA3.0 plasmids were used to achieve the multiplicity of infection (MOI) of 100, 200, and 300. The results indicate that all the cell lines with a MOI of 300 had the best transfection efficiency (the green fluorescence shows the transfected plasmids). Scale bar = 1,000  $\mu$ m. b) and c) Expression of *solute carrier family 20 member 2 (SLC20A2)*, as determined by b) quantitative real-time polymerase chain reaction (qRT-PCR) and c) western blot. There was no significant difference in *SLC20A2* expression level between the wild-type (WT) and mutant (MUT) groups. GAPDH, glyceraldehyde 3-phosphate dehydrogenase; mRNA, messenger RNA.

phosphorus metabolism, proliferation, and differentiation in ATDC5 chondrocytes.

## Methods

**Cell culture.** The ATDC5 cell line was purchased from American Type Culture Collection (ATCC, Manassas, Virginia, USA). The cells were grown in maintenance medium (named TS medium; Santa Cruz Biotechnology, Santa Cruz, California, USA), which was made of a 1:1 mixture of Dulbecco's Modified Eagle Medium (DMEM) and Ham's F-12 medium containing 1% (vol/vol) antibiotic-antimycotic, 5% fetal bovine serum (FBS), 10  $\mu$ g/ml human transferrin (T), and  $3 \times 10^{-8}$  mol/l sodium selenite (S). The cells were maintained in a humidified atmosphere of 5% CO<sub>2</sub> at 37°C. To induce differentiation, the ATDC5 cells were cultured in insulin-transferrin-selenium (ITS) medium (Santa Cruz Biotechnology), which was made of TS medium supplemented with 0.1 mg/ml insulin. After 14 days (D14) of ITS, the DMEM was substituted with Minimum Essential Medium  $\alpha$  ( $\alpha$ -MEM) until day 21 (D21).

**Construction of plasmids and transfection.** The mutation of *SLC20A2* (c.C1849T) was identified by whole-exome sequencing in a Chinese family with HME without EXT-1 and EXT-2 mutations.<sup>10</sup> The proband (age, four years; sex, male) sought medical advice at our hospital due to multiple exostoses at the bilateral distal femur, proximal tibia and fibula, distal tibia, proximal humerus, and left scapula. The mother and grandfather of the proband were also diagnosed with HME.<sup>10</sup>

The pcDNA3.0 plasmids were constructed by GenePharma (Shanghai, China). Since the ATDC5 cells are derived from mice, the corresponding mutation of *SLC20A2* in mice is C2343T (NM\_011394, GRCm38/mm10). The wild-type and mutant mouse *SLC20A2* complementary DNA (cDNA) (NM\_011394) were

cloned into the vector pcDNA3.0 (Thermo Fisher Scientific, Waltham, Massachusetts, USA) using NotI and HindIII restriction sites. Then, the pcDNA3.0 plasmids were collected, purified, and titered to ensure a titre greater than  $10^8$  TU/ $\mu$ l. Then, Sanger sequencing was used to confirm the cloned cDNAs (Figures 1a and 1b). The pcDNA3.0 plasmids were then transfected into ATDC5 cells using Lipofectamine 2000 (Invitrogen, Carlsbad, California, USA) according to the manufacturer's instructions.

ATDC5 cells transfected with pcDNA3.0 plasmids containing the wild-type *SLC20A2* gene and the mutated *SLC20A2* gene were named WT and MUT, respectively. Additionally, ATDC5 cells that were not transfected with the pcDNA3.0 plasmid were used as a control group.

**Quantitative real-time polymerase chain reaction.** The method of quantitative real-time polymerase chain reaction (qRT-PCR) was similar to that used in our previous study.<sup>27</sup> In brief, total RNA was extracted using TRIzol (Invitrogen, Rochester, New York, USA) according to the manufacturer's instructions and reverse transcribed into cDNA templates. The qRT-PCR reaction mixture contained 10  $\mu$ l of Bestar SybrGreen qPCR master Mix (DBI, Ludwigshafen, Germany), 0.5  $\mu$ l of each primer, 1  $\mu$ l of cDNA template, and 8  $\mu$ l of double-distilled water (ddH<sub>2</sub>O). The primers used in the present study were designed using Primer Express software (Applied Biosystems, Foster City, California, USA). Primer sequences are listed in Supplementary Table i. The amplification was conducted with a denaturation step at 94°C for two minutes, followed by 40 cycles of amplification at 94°C for 20 seconds, 58°C for 20 seconds, and 72°C for 20 seconds. The melting curve was analyzed between 62°C and 95°C. The relative messenger RNA (mRNA) levels of the genes were calculated using the

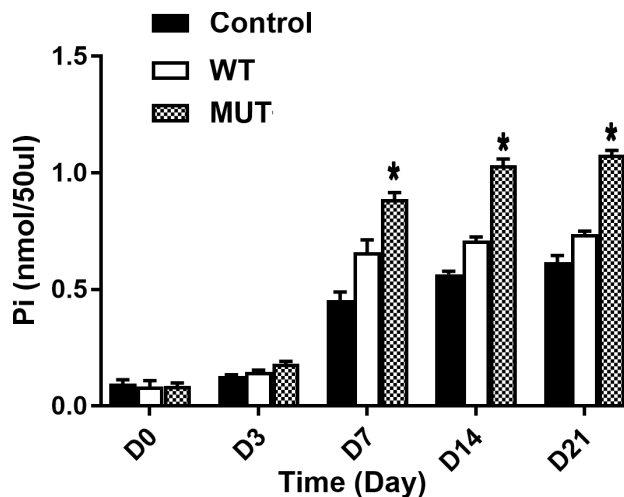


Fig. 3

The inorganic phosphate (Pi) concentration in the culture medium, as measured using a Malachite Green Phosphate Assay Kit and microplate spectrophotometer. A high Pi concentration in the medium reflected low Pi uptake in the cells. The Pi concentration in the mutant group (MUT) was significantly higher than that in the wild-type group (WT) on days 7, 14, and 21.

RT-PCR system (Mx3000P; Agilent Stratagene, Santa Clara, California, USA).

**Cell proliferation assay.** The method used for the cell proliferation assay was similar to that used in our previous study.<sup>27</sup> The proliferation of ATDC5 chondrocytes at different timepoints was determined using the Cell Counting Kit-8 (CCK-8) assay (Beyotime Biotechnology, Shanghai, China) according to the manufacturer's instructions. Briefly, CCK-8 solution (10  $\mu$ l/100  $\mu$ l medium) was added to the wells of each group and thoroughly mixed. Then, 100  $\mu$ l of CCK-8 medium was added to the cells and incubated at 37°C for four hours. The optical density (OD) values were detected with a microplate spectrophotometer (Thermo Fisher Scientific) at 450 nm.

**Western blotting analysis.** The method of western blotting analysis was similar to that used in our previous study.<sup>27</sup> ATDC5 chondrocytes were washed three times with phosphate-buffered saline (PBS) and then dissolved using 1% phenylmethylsulphonyl fluoride (PMSF) (Beyotime Biotechnology) for 30 minutes. The cells were centrifuged at 14,000 rpm for ten minutes, total protein was collected, and the concentrations were determined using a protein concentration determination kit (Thermo Fisher Scientific). Equal amounts of protein (30  $\mu$ g) from different samples were separated by 10% sodium dodecyl sulphate polyacrylamide gel electrophoresis (SDS-PAGE) at 80 V for 2.5 hours. The proteins were then transferred onto a polyvinylidene difluoride (PVDF) membrane (Millipore, Burlington, Massachusetts, USA). The membrane was rinsed with Tween-Tris buffered saline (TTBS) and blocked with a skim milk solution for one hour. The membranes were then incubated with primary antibodies against SLC20A2

(1:1000) (Abcam, Cambridge, UK), runt-related transcription factor 2 (Runx2) (1:1000; Abcam), aggrecan (Acan) (1:1000; Millipore),  $\alpha$ -1 chain of type II collagen (COL2A1) (1:1000; Santa Cruz Biotechnology), SRY-box transcription factor 9 (SOX9) (1:1000; Millipore),  $\alpha$ -1 chain of type X collagen (COL10A1) (1:1000; Santa Cruz, USA), matrix metalloproteinase 13 (MMP13) (1:1000; Abcam), Ihh (1:500; Abcam), PTHrP (1:1000; Abcam), and glyceraldehyde 3-phosphate dehydrogenase (GAPDH) (1:10000; Abcam) at 4°C overnight. The secondary horseradish peroxidase (HRP)-conjugated immunoglobulin G (IgG) antibody (1:2000; Boster Biological Technology, Pleasanton, California, USA) was added to the membranes after four washes with TTBS and incubated for 45 minutes at 37°C. The blots were developed using the ECL Plus reagent (Millipore), and images were recorded in the Gel Imaging System (Bio-Rad Laboratories, Hercules, California, USA).

**Alcian blue staining.** ATDC5 chondrocytes were plated in 12-well dishes and cultured in ITS differentiation medium for 21 days. The cells were rinsed with PBS, fixed for 30 minutes in 4% paraformaldehyde (Jianglaibio, Shanghai, China), and stained with an Alcian Blue solution (0.1% Alcian Blue in 0.1 M hydrochloric acid (HCl), pH 1; Sigma-Aldrich, St. Louis, Missouri, USA) overnight. Finally, the cells were washed twice with ddH<sub>2</sub>O and then dried. Images were taken using a Leica INM 200 UV microscope (Leica, Wetzlar, Germany). The area fraction of cartilage glycosaminoglycans was measured using ImageJ 1.51 v (National Institutes of Health (NIH), Bethesda, Maryland, USA).

**Alizarin red staining.** The culture medium was discarded, fixed with 4% paraformaldehyde for 15 to 20 minutes, and washed with PBS three times. Alizarin red staining solution (ScienCell, San Diego, California, USA) was prepared in advance and added to the culture plate. The plate was placed in the incubator for 15 minutes, and the staining solution was removed. The cells were washed with PBS solution three times and drained. Images were taken using a Leica INM 200 UV microscope. The area fraction of calcium deposition was measured using ImageJ 1.51 v (NIH).

**Malachite green-based assay for Pi determination.** The Pi concentration of the cells was determined by a Malachite Green Phosphate Assay Kit (Cayman Chemical, Ann Arbor, Michigan, USA) according to the manufacturer's instructions. Briefly, ATDC5 chondrocytes were cultured in ITS differentiation medium. On days 7, 14, and 21, 50  $\mu$ l of ITS medium from each group was collected before the medium was changed. The collected medium was then added to the 96-well Malachite Green Phosphate Assay Kit, and the developed malachite green-phosphomolybdate complex was measured with a microplate spectrophotometer (Thermo Fisher Scientific) at 620 nm.<sup>28</sup> The measured concentration of Pi in the medium could indirectly reflect the uptake of Pi by the cells. A high concentration of Pi in the medium reflected a low uptake of Pi in the cells.

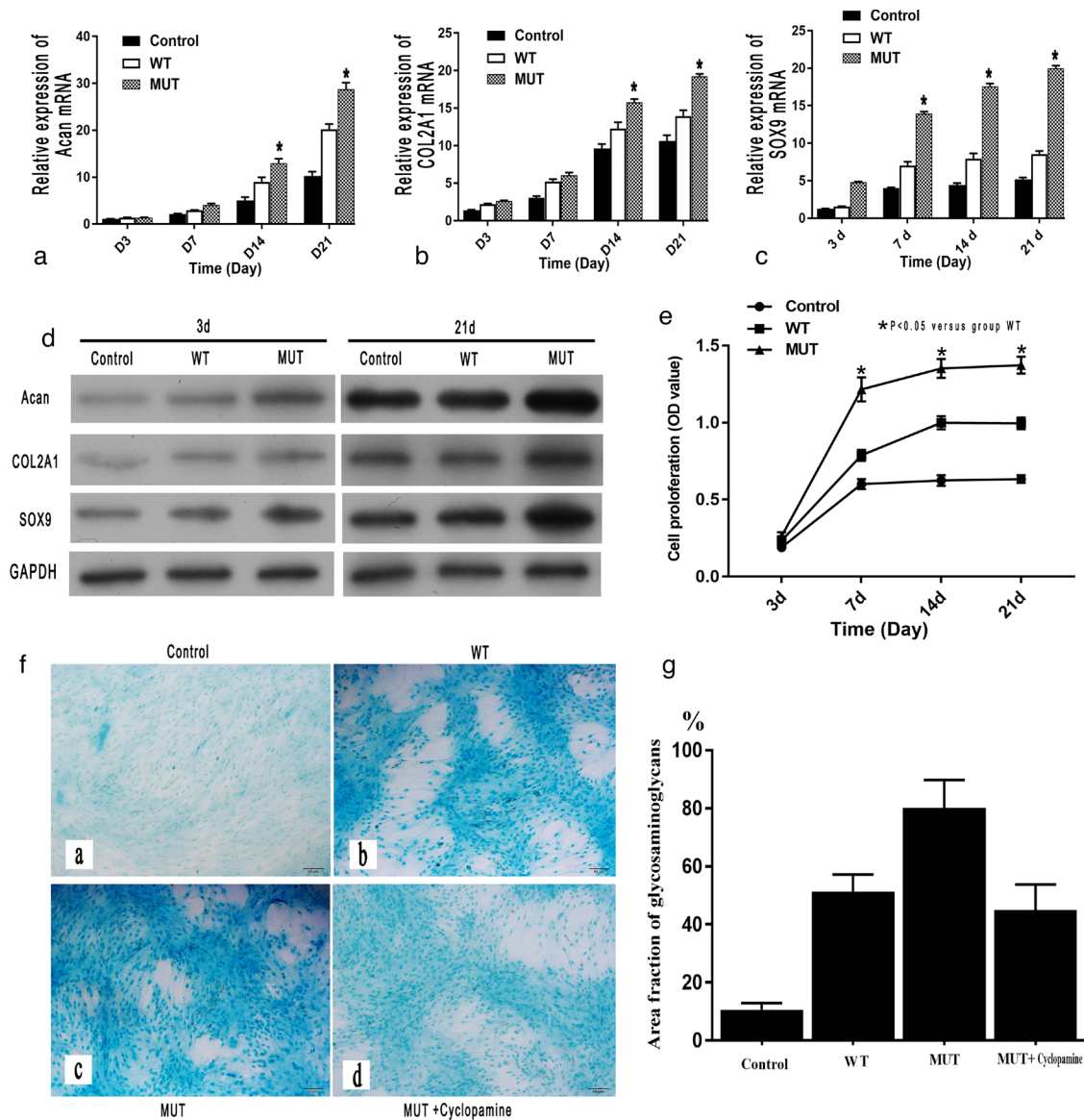


Fig. 4

The evaluation of cell proliferation of chondrocytes. The expression of markers of chondrocyte proliferation (aggrecan (Acan),  $\alpha$ -1 chain of type II collagen (COL2A1), and SRY-box transcription factor 9 (SOX9)), as measured by: a) to c) quantitative real-time polymerase chain reaction (qRT-PCR); and d) western blot, were significantly higher in the mutant (MUT) group than in the wild-type (WT) group. e) The proliferation rate (optical density (OD)) of the chondrocytes in the MUT group was significantly higher than that in the WT group on days 7, 14, and 21 ( $*p < 0.05$  vs WT group). f) and g) The results of Alcian blue staining (magnification: 100 $\times$ ) on day 21 also showed a significant increase of cartilage glycosaminoglycans (stained blue) in the MUT group when compared with the WT group. f) and g) Cyclopamine caused a decrease in cartilage glycosaminoglycans in the MUT group. Scale bar = 50  $\mu$ m. GAPDH, glyceraldehyde 3-phosphate dehydrogenase; mRNA, messenger RNA.

**Statistical analysis.** All data are expressed as means and SDs ( $n = 3$ ). One-way analysis of variance (ANOVA) and the least significant difference (LSD) post hoc test were used to evaluate the differences among groups. All statistical analyses were performed using the statistics package SPSS v22.0 (IBM, Armonk, New York, USA). A statistical value of  $p < 0.05$  was considered significant.

## Results

**Verification of the established ATDC5 cell lines.** An immunofluorescence examination was performed to

determine the transfection efficiency of the cell lines (WT and SLC20A2 mutation). Each cell line was transfected with three different quantities of pcDNA3.0 plasmids (10  $\mu$ l, 20  $\mu$ l, and 30  $\mu$ l; concentration =  $1 \times 10^8$  TU/ml). These three different quantities of plasmids could achieve a multiplicity of infection (MOI) of 100, 200, and 300, respectively. The results indicate that both cell lines had good transfection efficiency; however, the cell lines with an MOI of 300 had the best transfection efficiency (Figure 2a). Thus, we used these cell lines with an MOI of 300 for further investigation.

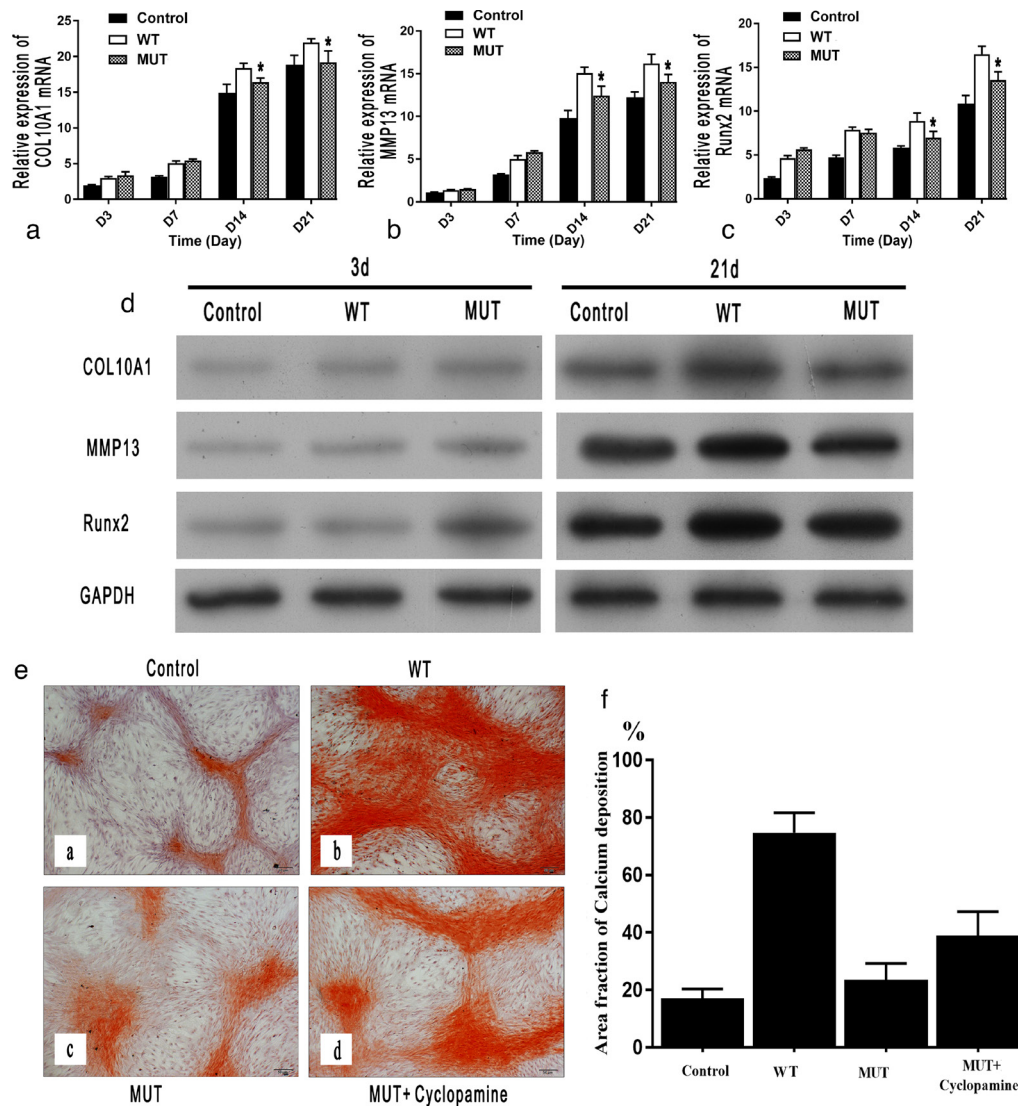


Fig. 5

The evaluation of chondrocyte differentiation. The expression of markers of chondrocyte differentiation ( $\alpha$ -1 chain of type X collagen (COL10A1), matrix metalloproteinase 13 (MMP13), and runt-related transcription factor 2 (Runx2)), as measured by: a) to c) quantitative real-time polymerase chain reaction (qRT-PCR); and d) western blot, were significantly lower in the mutant (MUT) group compared with the wild-type (WT) group. e) and f) The results of Alizarin red staining (magnification: 100 $\times$ ) on day 21 also showed that calcium deposition (stained red) was significantly decreased in the MUT group compared with the WT group, and cyclopamine caused a significant increase in calcium deposition in the MUT group. Scale bar = 50  $\mu$ m. GAPDH, glyceraldehyde 3-phosphate dehydrogenase; mRNA, messenger RNA.

**The expression of SLC20A2 was changed.** The expression level of *SLC20A2* was determined by qRT-PCR and western blot. Results of qRT-PCR indicate that the relative expression level of *SLC20A2* mRNA in cells with the *SLC20A2* mutation (MUT group) at day 14 was similar to that in WT cells (WT group) (Figure 2b). A similar result was obtained by western blot analysis (Figure 2c).

**SLC20A2 mutation induced lower uptake of Pi in ATDC5 chondrocytes.** The uptake of Pi in ATDC5 chondrocytes was determined by the Malachite Green Phosphate Assay Kit. The results indicate that the Pi concentration in the medium of cells with the *SLC20A2* mutation (MUT group) was significantly higher than that in the medium of WT group cells at days 7,

14, and 21 (Figure 3). In the present study, there was a basal Pi concentration in the culture medium. Thus, the higher concentration of Pi in the cells with *SLC20A2* meant that the *SLC20A2* mutation significantly inhibited Pi uptake in ATDC5 chondrocytes.

**SLC20A2 mutation significantly promoted chondrocyte proliferation.** The proliferation of ATDC5 differentiated chondrocytes at different timepoints was determined using the CCK-8 assay. We found that cells transfected with the mutated *SLC20A2* pcDNA3.0 plasmid (MUT group) exhibited a significantly greater proliferation rate at days 7, 14, and 21 than cells transfected with WT *SLC20A2* (WT group) (Figure 4e).

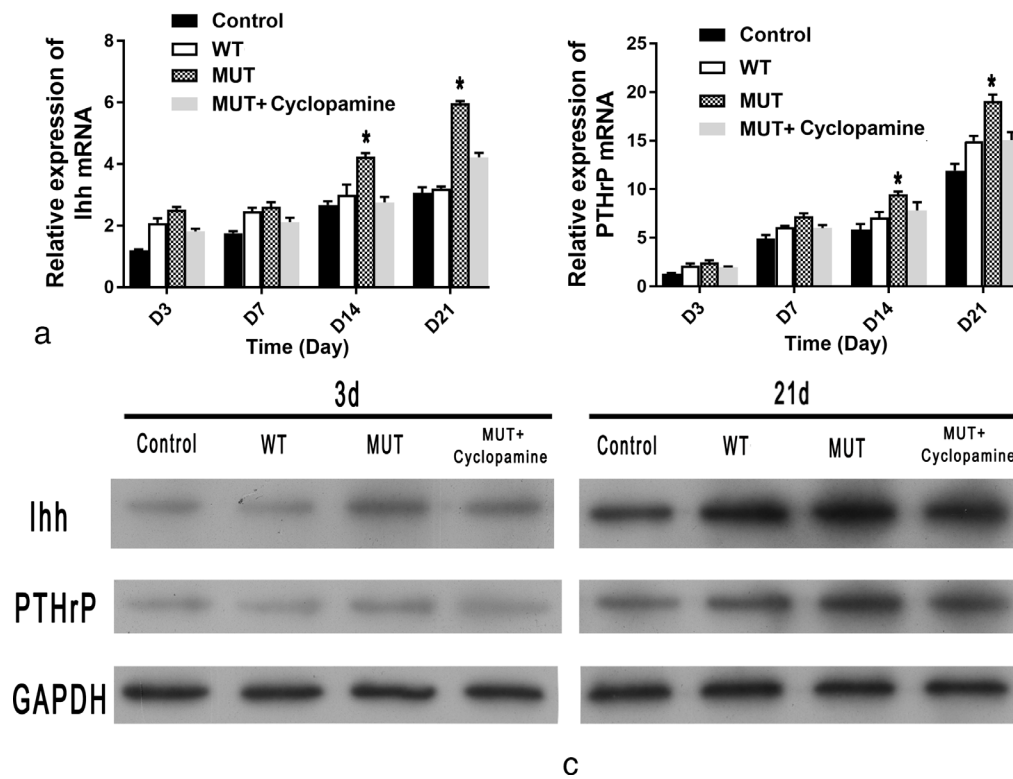


Fig. 6

The expression of Indian hedgehog (Ihh)/parathyroid hormone-related protein (PTHrP) signalling pathway. The expression of Ihh and PTHrP, as measured by: a) and b) quantitative real-time polymerase chain reaction (qRT-PCR); and c) western blot, were significantly higher in the mutant (MUT) group compared with the wild-type (WT) group. Cyclopamine significantly inhibited the expression of Ihh and PTHrP in the MUT group. GAPDH, glyceraldehyde 3-phosphate dehydrogenase; mRNA, messenger RNA.

The qRT-PCR results indicate that the relative mRNA expression of parameters of chondrocyte proliferation, such as *Acan*, *COL2A1*, and *SOX9*, in the MUT group was significantly higher than that in the WT group at days 7, 14, and 21 (Figures 4a to 4c). Similar results were obtained by western blot analysis (Figure 4d).

The results of Alcian blue staining showed that cartilage glycosaminoglycans were significantly more abundant in the MUT group than in the WT group at day 21 (Figures 4f and 4g).

**SLC20A2 mutation inhibited chondrocyte differentiation.** The results of qRT-PCR indicate that the relative mRNA expression of parameters of chondrocyte differentiation, such as *Runx2*, *COL10A1*, and *MMP13*, in the MUT group was significantly decreased compared to that in the WT group at days 14 and 21 (Figures 5a to 5c). Similar results were obtained by western blot analysis (Figure 5d).

Alizarin red staining showed that there was more calcium deposition in the WT group than in the MUT group (Figures 4e and 4f).

**SLC20A2 mutation activated the Ihh/PTHrP signalling pathway.** The qRT-PCR results indicate that the relative mRNA expression of Ihh and PTHrP in the MUT group was significantly higher than that in the WT group at days 7, 14, and 21 (Figures 6a and 6b). Similar results

were obtained by western blot analysis at day 21 (Figure 6c). An inhibitor (cyclopamine) of the Ihh/PTHrP signalling pathway significantly inhibited the proliferation (Figures 4f and 4g) and restored the differentiation of chondrocytes (Figures 5e and 5f) in the MUT group, as shown by Alizarin red and Alcian blue staining.

## Discussion

PiT-2 is widely expressed in all kinds of tissues and organs, including chondrocytes.<sup>12,13,29</sup> In the present study, mutations in *SLC20A2* did not lead to a significant change in the expression level of PiT-2 in ATDC5 chondrocytes (Figures 2b and 2c). At present, no study has reported the effect of gene mutation on the expression of *SLC20A2* in chondrocytes. However, Taglia et al<sup>30</sup> investigated the effect of the *SLC20A2* mutation on PiT-2 expression in patient fibroblasts and found that the mutation did not affect PiT-2 expression. However, some other studies reported a decrease in *SLC20A2* mRNA by approximately 10% to 35% in cells from affected patients.<sup>31-33</sup> The expression of *SLC20A2* did not significantly decrease in the present study, which may be attributed to the location of the mutation. In theory, the mutation in *SLC20A2* (c.C1849T) may lead to a change in the amino acid sequence (p.R617C) (Figures 1c and 1d), in which

the 617<sup>th</sup> amino acid (arginine) is changed to cysteine. This mutation was not a truncation mutation, and it did not lead to a stop of mRNA translation. Additionally, the relative molecular masses of arginine (174.2) and cysteine (121.1) were similar, leaving the expression level of *SLC20A2* unchanged.

Although the expression of *SLC20A2* did not change significantly, the function of PiT-2 was influenced. The present study shows significantly decreased uptake of Pi in ATDC5 chondrocytes with the *SLC20A2* mutation. Since PiT-2 is a NaPi-III cotransporter that mediates the transmembrane movement of sodium and Pi, the changed function of PiT-2 may contribute to the decrease in Pi uptake. Our previous study showed that the mutation of *SLC20A2* (c.C1849T) was at the highly conserved amino acid sequences, at which a mutation might have a great probability to induce structural and functional changes.<sup>10</sup> Other studies have also reported severe Pi transport impairment in cells with *SLC20A2* mutations.<sup>30,34,35</sup> In particular, in the study by Taglia et al<sup>30</sup> mentioned above, although the authors did not find significant changes in PiT-2 expression in *SLC20A2* mutant cells, they observed significantly reduced Pi uptake, which may be attributed to altered PiT-2 subcellular localization in cells with the *SLC20A2* mutation.

Our study also indicates that the *SLC20A2* mutation promotes chondrocyte proliferation while inhibiting chondrocyte differentiation. Chondrocytes with the *SLC20A2* mutation exhibited a significantly greater proliferative rate than cells with WT *SLC20A2* (Figure 4f). The expression of markers of chondrocyte proliferation (Acan, COL2A1, and SOX9) were significantly increased in ATDC5 chondrocytes with the *SLC20A2* mutation. The Alcian blue staining also showed similar results (Figure 4f). In contrast, the expression of markers of chondrocyte differentiation (Runx2, COL10A1, and MMP13) and calcium deposition (Figure 5) were significantly decreased in ATDC5 chondrocytes with the *SLC20A2* mutation. These results may be attributed to the decreased uptake of Pi in cells with the *SLC20A2* mutation. Studies have demonstrated that Pi plays an important role in chondrocyte differentiation, maturation, and mineralization, and all these effects are dependent on Pi entry into cells through sodium-dependent transporters.<sup>36-38</sup> Liu et al<sup>39</sup> cultured mouse metatarsals with low Pi medium (0.05 mM) and found significantly impaired chondrocyte differentiation compared with that of the control group. In contrast, Zalutskaya et al<sup>19</sup> cultured mouse metatarsals in high Pi medium (7 mM) and found that compared with low Pi (1.25 mM), high Pi significantly decreased chondrocyte proliferation and promoted chondrocyte differentiation. Other studies have also reported that Pi enhances chondrocyte differentiation and maturation.<sup>36,40</sup> Our results agreed with previous studies.<sup>36-40</sup> Studies have found that HME is characterized by inappropriate chondrocyte proliferation and bone growth arising at the juxtaepiphyseal

region of long bones,<sup>17,18</sup> thus the results of our study point to a new direction of the mechanism of development of HME in patients without mutation of *EXT1* or *EXT2*. Furthermore, the mutation of *SLC20A2* might lead to the development of HME by inducing a disturbance of proliferation and differentiation of chondrocyte.

Our study also shows that the *Ihh*/PTHrP signalling pathway plays an important role in *SLC20A2* mutation-induced disturbance of chondrocyte proliferation and differentiation. The expression of *Ihh* and PTHrP was significantly higher in ATDC5 chondrocytes with the *SLC20A2* mutation. It has been demonstrated that *Ihh* acts through PTHrP, and activation of *Ihh* signalling upregulates PTHrP while preventing chondrocyte hypertrophy.<sup>41</sup> Minina et al<sup>22</sup> found that overexpression of *Ihh* inhibited hypertrophic differentiation of chondrocytes, and it could be recovered by an inhibitor of the *Ihh* signalling pathway (cyclopamine). Additionally, other studies have demonstrated that Pi and PTHrP are required for normal growth plate maturation, and the PTH/PTHrP receptor mediates the effects of *Ihh* and PTHrP on chondrocyte differentiation.<sup>39,42</sup> Liu et al<sup>39</sup> found that low Pi significantly increased PTHrP expression while attenuating chondrocyte differentiation in cultured metatarsals; however, low Pi did not impair chondrocyte differentiation in PTHrP knockout mice. Our results agreed with previous studies.<sup>22,39,42</sup> When an inhibitor of the *Ihh* signalling pathway (cyclopamine) was added, the expression of PTHrP and *Ihh* and chondrocyte proliferation (Figures 4f and 4g) was decreased as expected, while the chondrocyte differentiation of cells with the *SLC20A2* mutation partially recovered (Figures 5e and 5f).

It should be noted that there are some limitations in the present study. We only used cell models to investigate the effect of *SLC20A2* mutation (c.C1849T) on the proliferation and differentiation of chondrocytes, and we used a transfection system which meant that *SLC20A2* would be overexpressed in all cells. However, we do not think this changes the conclusion. Since both groups (WT and MUT) were overexpressed, all of them have a same base level of expression of *SLC20A2* which makes them comparable.

In conclusion, a mutation in *SLC20A2* (c.C1948T) does not change the expression of *SLC20A2*. However, it leads to decreased Pi uptake in ATDC5 chondrocytes. *SLC20A2* mutation also promotes chondrocyte proliferation while inhibiting chondrocyte differentiation. The *Ihh*/PTHrP signalling pathway may play an important role in the *SLC20A2* mutation-induced disturbance of chondrocyte proliferation and differentiation. The present study points to a new direction to investigate the mechanism of development of HME in patients without mutation of *EXT1* or *EXT2*. The mutation of *SLC20A2* might lead to the development of HME by inducing a disturbance of proliferation and differentiation of chondrocytes.

## Supplementary material



Table showing the primer sequences used in real-time polymerase chain reaction.

## References

- Beltrami G, Ristori G, Scoccianti G, et al. Hereditary multiple exostoses: a review of clinical appearance and metabolic pattern. *Clin Cases Miner Bone Metab.* 2016;13(2):110–118.
- McFarlane J, Knight T, Sinha A, et al. Exostoses, enchondromatosis and metachondromatosis; diagnosis and management. *Acta Orthop Belg.* 2016;82(1):102–105.
- Pacifici M. Hereditary multiple exostoses: new insights into pathogenesis, clinical complications, and potential treatments. *Curr Osteoporos Rep.* 2017;15(3):142–152.
- De Mattos CBR, Binitie O, Dormans JP. Pathological fractures in children. *Bone Joint Res.* 2012;1(10):272–280.
- Wuyts W, Radersma R, Storm K, Vits L. An optimized DHPLC protocol for molecular testing of the EXT1 and EXT2 genes in hereditary multiple osteochondromas. *Clin Genet.* 2005;68(6):542–547.
- Santos SCL, Rizzo IMPO, Takata RI, et al. Analysis of mutations in EXT1 and EXT2 in Brazilian patients with multiple osteochondromas. *Mol Genet Genomic Med.* 2018;6(3):382–392.
- Sarrion P, Sangorrin A, Urreiziti R, et al. Mutations in the EXT1 and EXT2 genes in Spanish patients with multiple osteochondromas. *Sci Rep.* 2013;3:1346.
- Xu L, Xia J, Jiang H, et al. Mutation analysis of hereditary multiple exostoses in the Chinese. *Hum Genet.* 1999;105(1-2):45–50.
- Ishimaru D, Gotoh M, Takayama S, et al. Large-scale mutational analysis in the EXT1 and EXT2 genes for Japanese patients with multiple osteochondromas. *BMC Genet.* 2016;17:52.
- Li Y, Lin X, Zhu M, et al. Whole-exome sequencing identifies a novel mutation of SLC20A2 (c.C1849T) as a possible cause of hereditary multiple exostoses in a Chinese family. *Mol Med Rep.* 2020;22(3):2469–2477.
- Forster IC, Hernando N, Biber J, Murer H. Phosphate transporters of the SLC20 and SLC34 families. *Mol Aspects Med.* 2013;34(2-3):386–395.
- Solomon DH, Wilkins RJ, Meredith D, Browning JA. Characterisation of inorganic phosphate transport in bovine articular chondrocytes. *Cell Physiol Biochem.* 2007;20(1-4):99–108.
- Virkki LV, Biber J, Murer H, Forster IC. Phosphate transporters: a tale of two solute carrier families. *Am J Physiol Renal Physiol.* 2007;293(3):F643–F654.
- Collins JF, Bai L, Ghishan FK. The SLC20 family of proteins: dual functions as sodium-phosphate cotransporters and viral receptors. *Pflugers Arch.* 2004;447(5):647–652.
- Sekine S-I, Nishii K, Masaka T, et al. SLC20A2 variants cause dysfunctional phosphate transport activity in endothelial cells induced from idiopathic basal ganglia calcification patients-derived iPSCs. *Biochem Biophys Res Commun.* 2019;510(2):303–308.
- Lemos RR, Ramos EM, Legati A, et al. Update and mutational analysis of SLC20A2: a major cause of primary familial brain calcification. *Hum Mutat.* 2015;36(5):489–495.
- Duke PJ, Montufar-Solis D, Haynes R, Hecht JT. Ultrastructural abnormalities in cultured exostosis chondrocytes. *Ultrastruct Pathol.* 2002;26(2):99–106.
- Benoist-Lasselien C, de Margerie E, Gibbs L, et al. Defective chondrocyte proliferation and differentiation in osteochondromas of MHE patients. *Bone.* 2006;39(1):17–26.
- Zalutskaya AA, Cox MK, Demay MB. Phosphate regulates embryonic endochondral bone development. *J Cell Biochem.* 2009;108(3):668–674.
- Khoshniat S, Bourguine A, Julien M, et al. The emergence of phosphate as a specific signaling molecule in bone and other cell types in mammals. *Cell Mol Life Sci.* 2011;68(2):205–218.
- Ma RS, Zhou ZL, Luo JW, et al. The Ihh signal is essential for regulating proliferation and hypertrophy of cultured chicken chondrocytes. *Comp Biochem Physiol B Biochem Mol Biol.* 2013;166(2):117–122.
- Minina E, Wenzel HM, Kreschel C, et al. Bmp and Ihh/PTHrP signaling interact to coordinate chondrocyte proliferation and differentiation. *Development.* 2001;128(22):4523–4534.
- Lai LP, Mitchell J. Indian hedgehog: its roles and regulation in endochondral bone development. *J Cell Biochem.* 2005;96(6):1163–1173.
- Chen Z, Zhang Z, Guo L, et al. The role of histone deacetylase 4 during chondrocyte hypertrophy and endochondral bone development. *Bone Joint Res.* 2020;9(2):82–89.
- Yao Y, Wang Y. Atdc5: an excellent in vitro model cell line for skeletal development. *J Cell Biochem.* 2013;114(6):1223–1229.
- Shukunami C, Ishizeki K, Atsumi T, et al. Cellular hypertrophy and calcification of embryonal carcinoma-derived chondrogenic cell line ATDC5 in vitro. *J Bone Miner Res.* 1997;12(8):1174–1188.
- Li Y, Li J, Zhou Q, et al. Mtorc1 signaling is essential for neurofibromatosis type I gene modulated osteogenic differentiation of BMSCs. *J Cell Biochem.* 2019;120(3):2886–2896.
- Baykov AA, Evtushenko OA, Avaeva SM. A malachite green procedure for orthophosphate determination and its use in alkaline phosphatase-based enzyme immunoassay. *Anal Biochem.* 1988;171(2):266–270.
- Orfanidou T, Malizos KN, Varitimidis S, Tsezou A. 1,25-Dihydroxyvitamin D(3) and extracellular inorganic phosphate activate mitogen-activated protein kinase pathway through fibroblast growth factor 23 contributing to hypertrophy and mineralization in osteoarthritic chondrocytes. *Exp Biol Med.* 2012;237(3):241–253.
- Taglia I, Formichi P, Battisti C, et al. Primary familial brain calcification with a novel SLC20A2 mutation: analysis of Pit-2 expression and localization. *J Cell Physiol.* 2018;233(3):2324–2331.
- Zhang Y, Guo X, Wu A. Association between a novel mutation in SLC20A2 and familial idiopathic basal ganglia calcification. *PLoS One.* 2013;8(2):e57060.
- Mi T-M, Mao W, Cai Y-N, et al. Primary familial brain calcifications linked with a novel SLC20A2 gene mutation in a Chinese family. *J Neurogenet.* 2017;31(3):149–152.
- Ferreira JB, Pimentel L, Keasey MP, et al. First report of a de novo mutation at SLC20A2 in a patient with brain calcification. *J Mol Neurosci.* 2014;54(4):748–751.
- Botzger P, Pedersen L. Two highly conserved glutamate residues critical for type III sodium-dependent phosphate transport revealed by uncoupling transport function from retroviral receptor function. *J Biol Chem.* 2002;277(45):42741–42747.
- Salaün C, Maréchal V, Heard JM. Transport-deficient Pit2 phosphate transporters still modify cell surface oligomers structure in response to inorganic phosphate. *J Mol Biol.* 2004;340(1):39–47.
- Magne D, Bluteau G, Fauchoux C, et al. Phosphate is a specific signal for ATDC5 chondrocyte maturation and apoptosis-associated mineralization: possible implication of apoptosis in the regulation of endochondral ossification. *J Bone Miner Res.* 2003;18(8):1430–1442.
- Mansfield K, Teixeira CC, Adams CS, Shapiro IM. Phosphate ions mediate chondrocyte apoptosis through a plasma membrane transporter mechanism. *Bone.* 2001;28(1):1–8.
- Meleti Z, Shapiro IM, Adams CS. Inorganic phosphate induces apoptosis of osteoblast-like cells in culture. *Bone.* 2000;27(3):359–366.
- Liu ES, Zalutskaya A, Chae BT, et al. Phosphate interacts with PTHrP to regulate endochondral bone formation. *Endocrinology.* 2014;155(10):3750–3756.
- Miedlich SU, Zalutskaya A, Zhu ED, Demay MB. Phosphate-Induced apoptosis of hypertrophic chondrocytes is associated with a decrease in mitochondrial membrane potential and is dependent upon ERK1/2 phosphorylation. *J Biol Chem.* 2010;285(24):18270–18275.
- Karp SJ, Schipani E, St-Jacques B, et al. Indian hedgehog coordinates endochondral bone growth and morphogenesis via parathyroid hormone related-protein-dependent and -independent pathways. *Development.* 2000;127(3):543–548.
- Lanske B, Karaplis AC, Lee K, et al. Pth/PTHrP receptor in early development and Indian hedgehog-regulated bone growth. *Science.* 1996;273(5275):663–666.

### Author information:

- Y. Li, MD, Attending Doctor
- X. Lin, PhD, Resident Doctor
- M. Zhu, PhD, Professor, Researcher
- F. Xun, MD, Technician
- J. Li, MD, Attending Doctor
- Z. Yuan, MD, Attending Doctor
- Y. Liu, MD, Attending Doctor
- H. Xu, PhD, Chief Surgeon, Head of Department  
Department of Pediatric Orthopaedics, Guangzhou Women and Children's Medical Center, Guangzhou Medical University, Guangzhou, China.

### Author contributions:

- Y. Li: Conceptualized and supervised the study, Performed the methodology, Wrote, reviewed, edited, and approved the manuscript, Acquired the funding, Analyzed the data.
- X. Lin: Conceptualized and supervised the study, Performed the methodology, Wrote, reviewed, edited, and approved the manuscript.
- M. Zhu: Conducted the experimental investigations, Read and approved the manuscript.
- F. Xun: Conducted the experimental investigations, Read and approved the manuscript.
- J. Li: Conducted the experimental investigations, Read and approved the manuscript.

- Z. Yuan: Conducted the experimental investigations, Read and approved the manuscript.
- Y. Liu: Conducted the experimental investigations, Read and approved the manuscript.
- H. Xu: Conceptualized and supervised the study, Performed the methodology, Wrote, reviewed, edited, and approved the manuscript, Conducted the experimental investigations.

**Funding statement:**

- This work was supported by the National Nature Science Foundation of China, grant number No. 81702116. No benefits in any form have been received or will be received from a commercial party related directly or indirectly to the subject of this article.

**Ethical review statement**

- The study protocol was approved by the Human Ethics Committee of the Guangzhou Women and Children's Medical Center and Guangzhou Medical University (No. 2017-320). All patients signed informed consent forms. In the case of children, written or verbal informed consent to participate was obtained from the parents.

© 2020 Author(s) et al. This is an open-access article distributed under the terms of the Creative Commons Attribution Non-Commercial No Derivatives (CC BY-NC-ND 4.0) licence, which permits the copying and redistribution of the work only, and provided the original author and source are credited. See <https://creativecommons.org/licenses/by-nc-nd/4.0/>.